

Cyclone and monsoonal wave characteristics of northwestern Bay of Bengal: long-term observations and modeling

Sisir Kumar Patra¹ · Pravakar Mishra² · P. K. Mohanty³ ·
U. K. Pradhan² · U. S. Panda² · M. V. Ramana Murthy² ·
V. Sanil Kumar⁴ · T. M. Balakrishnan Nair⁵

Received: 30 July 2015 / Accepted: 5 February 2016 / Published online: 18 February 2016
© Springer Science+Business Media Dordrecht 2016

Abstract Long-term wave data play a crucial role in arriving the wave criteria for ports and harbors and shore protection structures. Seasonal and annual wave characteristics are studied based on wave data collected for the year 1994, 2008–2009 and 2013–2014 off Gopalpur, northwestern Bay of Bengal (BoB). The tropical cyclones ensued in BoB hit the coast frequently causing severe erosion due to extreme waves. The sea and swell waves are separated by wave steepness method, and the significant wave height (H_s), zero-crossing period and mean wave direction are examined. The results indicate a distinct shift in sea direction by 90° during mid-November to mid-February compared with rest of the year. Throughout the year, predominant swell direction is 160° . In an annual cycle, the contribution of swells in wave height is slightly higher than that of the seas. Annual occurrences of single-, double- and multi-peaked spectra are 22, 40 and 38 %, respectively. The waves are predominant southerly during the southwest monsoon (June, July, August and September) and south-southeasterly for rest of the year, and the variations of wave parameters for three different years are trivial. The spectral wave model MIKE 21 is used to simulate wave characteristics using reanalyzed NCEP wind data for the period June 2008 to May 2009 which exhibits good agreement with a correlation coefficient (R) of 0.86 for H_s . The design significant wave height of 7.1 m and 7.8 m is calculated for 10 and 100 years of return periods, respectively, by Weibull distribution.

Keywords Monsoonal wave · Sea and swell · Spectral wave model · Bay of Bengal

✉ Pravakar Mishra
mishra@icmam.gov.in

¹ National Institute of Ocean Technology (NIOT), Pallikaranai, Chennai 600100, India

² ICMAM-Project Directorate, NIOT Campus, Pallikaranai, Chennai 600100, India

³ Berhampur University, Berhampur, Odisha 760007, India

⁴ National Institute of Oceanography, Dona Paula, Goa 403004, India

⁵ Indian National Centre for Ocean Information Services (INCOIS), Hyderabad 500055, India

1 Introduction

Waves are dominant features in the coastal zones; knowledge on its characteristics is essential for the designing of coastal projects, shore protection measures and other civil and military coastal activities (Coastal Engineering Manual 2008). Waves generated by the wind are complex, consisting of superimposed multitude of components of varying heights and periodicity (Sorensen 2006). As the sea state is composed of locally generated seas and swells of distant storms, the wave energy spectra often show two or more spectral peaks corresponding to different generating sources (Hanson and Phillips 1999). Identification and separation of sea and swell provide a realistic depiction of the sea state and are of great importance to both scientific and engineering applications (Wang and Hwang 2001).

The incidence of tropical cyclone is a regular feature in pre-monsoon (May) and post-monsoon (October and November) over Bay of Bengal (BoB) and experiences three to six tropical cyclones (TC) annually, with increase in the intensity (Alam et al. 2003; Mohapatra and Mohanty 2004; Balaguru et al. 2014). The semi-enclosed northern BoB basin with shallow continental shelf, low-lying flat coastal terrain and high population density increases the societal importance despite lower TC formation rate in the BoB compared with Atlantic and Pacific basins (Webster 2008; Islam and Peterson 2009; Mcphaden et al. 2009). Storm-generated wave, coupled with locally generated wind, creates complex characteristics in the nearshore region and primarily causes erosion (loss of sediment) and increase in sea level (storm surge), which are threats to the life and wealth of the coastal community (Rao et al. 2007; Amrutha et al. 2014). Therefore, the wave characteristics during cyclone need to be accessed carefully due to its severity.

Wave modeling provides information of wave propagation across the continental shelf to the nearshore area. Observations along Indian coast indicate that the generation, growth and decay of wind waves are generally congruent with the prevailing wind regime and their seasonality; variability in the wave spectrum at a given site depends on the frequency and intensity of tropical storms that contributes to the regional wave climate considerably (Glejin et al. 2013; Kumar et al. 2014). Kumar et al. (2003) have reported that about 60 % of the wave spectra are multi-peaked, sea-dominated double-peaked wave spectra were seen during June to September, and single-peaked spectra are observed mostly when the significant wave height (H_s) is more than 2 m. Aboobacker et al. (2009) reported the existence of seas along with ‘Young’ swells in BoB, and single-peaked spectra are observed during extreme events, wherein all the energies are concentrated in low-frequency region.

The design of offshore or coastal structures usually takes a reference of the maximum wave height during storms so that structures can withstand for many years. The parameter chosen to describe such conditions is wave height with 50- to 100-year return value. As the coast experiences 3–6 tropical cyclones every year, the design wave height estimate is a prerequisite for port and coastal development activities.

Gopalpur is located along northwestern part of Bay of Bengal, a fairly straight coastline with an orientation of 48°E to north (Fig. 1). The weather is primarily governed by monsoons and rough sea-state conditions experienced during low-pressure systems, cyclones in BoB (Mishra et al. 2011). During 1987, an open-coast port was constructed by excavating the backshore and connecting it through a 250-m-wide channel. Usually, ships are anchored at midstream at a distance of 2 km from the shore, and cargo was loaded and discharged through lighters, and two piers are constructed for dredging and handling cargos. Since 2007, the port is under renovation to an all-weather open seaport. As long-term wave data collection is limited, expensive and logistically difficult, wave data

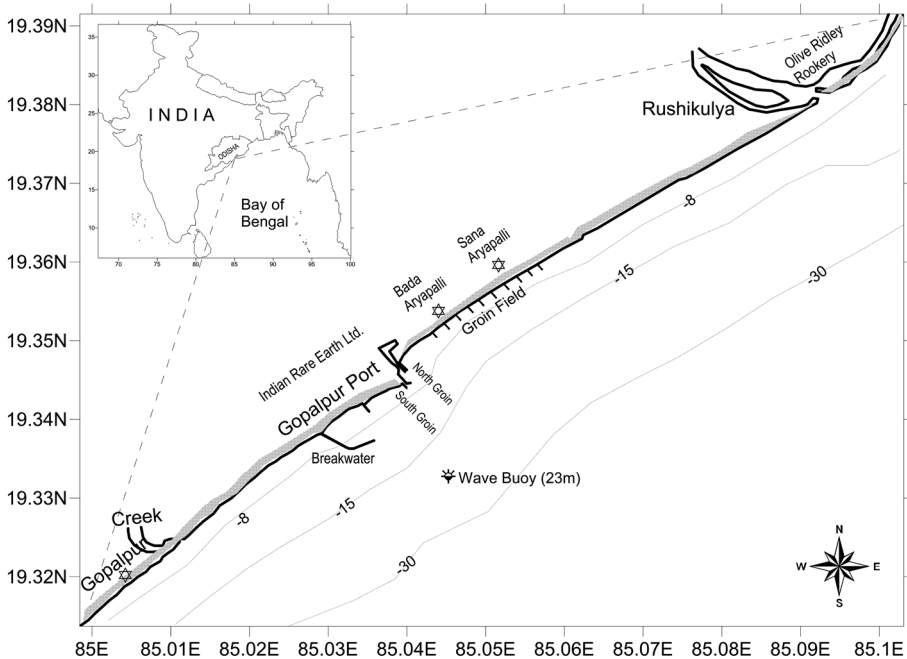


Fig. 1 Map showing the study area and wave buoy deployment location

collected for selected periods (1994, 2008–2009 and 2013–2014) during the last two decades are evaluated for the annual and inter-annual wave climate distribution, monthly and seasonal sea and swell characteristics and sea state during cyclones for design of coastal structures and from other shoreline management point of view (Kumar et al. 2003; Mishra et al. 2011; Murty et al. 2014). The nearshore wave climate is estimated using the spectral wave model (DHI 2011) and validated with the observed wave data.

2 Materials, methods and models

2.1 Data

Wave observations off Gopalpur ($19^{\circ}15.5'N$ and $84^{\circ}54.4'E$) at 23 m water depth from June 1, 2008, to May 31, 2009, are made using Datawell directional waverider buoy (Datawell 2006). The data are recorded for 30-min duration at every one-hour interval and sampled at a frequency of 1.28 Hz. Past wave data for Gopalpur (~ 15 m depth) were obtained from National Institute of Oceanography (NIO), Goa, for one year during January to December 1994 (Kumar et al. 2003). Similarly, wave data for the period June 2013 to May 2014 are obtained from the ongoing wave watch program for Gopalpur (at a depth of ~ 12 m) through INCOIS, Hyderabad (Murty et al. 2014). The wave parameters, viz. maximum wave height (H_{max}), significant wave height (H_s), zero-crossing wave period (T_z) and wave period corresponding to maximum spectral energy (T_p), are obtained through spectral analysis. Wave data of three different time periods are compiled to assess the monthly, seasonal and inter-annual variabilities.

The information on cyclone parameters is collected from Indian Meteorological Department (IMD), New Delhi. The water level variations were recorded at Gopalpur port for June 2008 to May 2009 using a Valeport tide gauge, and harmonic analysis was performed to estimate the tidal and non-tidal (surge) component (Mishra et al. 2014).

2.2 Methods

The separation of sea and swell components from the wave spectra for the period June 2008 to May 2009 was derived following standard wave steepness method of National Data Buoy Center (Gilhousen and Hervey 2001). Estimations are made by selecting a separation frequency f_s that partitions the wave spectrum into its sea and swell parts and their components, viz. significant wave height (H_{sw} and H_{ss}), zero-crossing period (T_{sw} and T_{ss}) and mean wave direction (θ_{sw} and θ_{ss}). The steepness function $\zeta(f)$ and separation frequency f_s are given by Eqs. 1 and 2.

$$\zeta(f) = \frac{8\pi m_2(f)}{g\sqrt{m_0(f)}} \quad (1)$$

$$f_s = Cf_m \quad (2)$$

where f_m is the frequency of maximum of $\zeta(f)$, g is the acceleration due to gravity, m_0 and m_2 are the zero- and second-order spectral moments and $C = 0.75$ is empirically determined constant (Gilhousen and Hervey 2001).

Extreme value analysis was performed following Weibull probability distribution using statistical model MAVE_FIT (SANDS 2013) to predict the values for the selected return periods. In this model, the parameters of the parametric distribution functions are estimated from sets of observations by applying the maximum likelihood estimation (MLE) technique. These probability distribution functions (PDF) are assumed to be the parent distributions of the observations in terms of the probability that, for a random event, the stochastic variable x does not exceed the value x .

2.3 Model setup

The MIKE 21 Spectral Wave Model of DHI is a third-generation spectral wind wave model based on unstructured meshes. The model simulates the growth, decay and transformation of wind-generated waves and swells in offshore and coastal areas. It includes the wave growth by action of wind, nonlinear wave–wave interaction, dissipation due to whitecapping, dissipation due to bottom friction, dissipation due to depth-induced wave breaking, refraction and shoaling due to depth variations, wave–current interaction, effect of time-varying water depth and flooding and drying.

The model is based on numerical integration of wave action balance equation formulated in Cartesian coordinates (Komen et al. 1996; Young 1999). The discretization of the governing equation in geographical and spectral space is performed using cell-centered finite volume method. In the geographical domain, an unstructured mesh technique is used. The details of the model equations and their solution are explained in DHI user manual (2011). The bathymetry of the study area was prepared using the observed nearshore (up to 20 m) echo sounding data, the ETOPO1 (Earth Topography—1 min) and MIKE C-Map data (Fig. 2). The model is executed using NCEP (2009) winds with a resolution of $2.5^\circ \times 2.5^\circ$ at every 6-h interval.

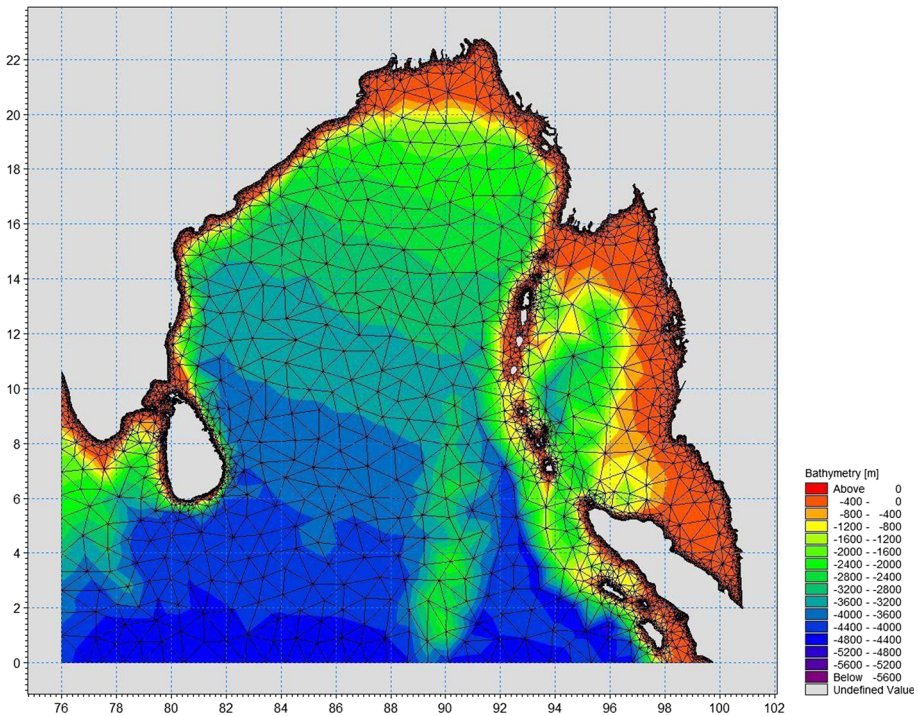


Fig. 2 Model domain and bathymetry used for study

3 Results and discussion

A number of studies describing the annual wave climate, sea and swell characteristics and their seasonality for east coast India are available (Sundar 1986; Chandramohan et al. 1988; Chauhan 1995; Kumar et al. 2003, 2008, 2014; Suresh et al. 2010; Aboobacker et al. 2011; Amrutha et al. 2014). Mostly, the nearshore wave characteristics of western BoB are described under the following three seasons, viz. southwest monsoon (June to September), post-monsoon (October to December) and non-monsoon or the fair weather period (January to May). However, based on the observed wave variability for Gopalpur, we regrouped the data under four categories, viz. southwest (SW) monsoon (June to September), post-monsoon (October and November), fair weather (December to February) and pre-monsoon (March to May). The wave intensity is high during SW monsoon, low in post-monsoon, very low during fair weather and moderate during pre-monsoon (Mishra et al. 2011).

3.1 Observed wind and wave off Gopalpur during 2008–2009

Wind and wave data for the period 2008–2009 are analyzed to understand the land–sea breeze interactions on prevailing wave characteristics and their intra- and inter-annual variabilities. Table 1 shows the range and mean values for wind speed, wave heights (H_{\max} , H_s , H_{sw} and H_{ss}), wave periods (T_z , T_{sw} , T_{ss} and T_p), spectral energy (E_{\max}), width (ϵ), narrowness (ν) and peakedness (Q_p) parameters. Maximum wave height (H_{\max}) of the order of 5.22 and 5.37 m was observed on July 29 and August 11, 2008. In addition to this,

Table 1 Minimum, maximum and mean values for wind and wave parameters observed during 2008–2009

Parameters	Minimum	Maximum	Average
Wind speed (m/s)	0.10	17.91	2.91
Maximum wave height, H_{\max} (m)	0.48	5.37	1.59
Significant wave height, H_s (m)	0.26	3.29	1.06
Significant sea wave height, H_{ss} (m)	0.12	2.08	0.72
Significant swell wave height, H_{sw} (m)	0.12	2.84	0.72
Mean wave period, T_z (s)	2.63	13.76	5.62
Peak wave period, T_p (s)	2.2	20	11.16
Maximum spectral energy, E_{\max} (m^2/Hz)	0.04	30.64	1.48
Spectral width parameter (ϵ)	0.53	0.96	0.8
Spectral narrowness parameter (ν)	0.33	1	0.59
Spectral peakedness parameter (Q_p)	1	8.5	1.84

H_{\max} exceeding 4 m was also noticed during September 2008, November 2008 and May 2009 coinciding with cyclonic events in BoB, i.e., depression (September 16–18, 2008), KhaiMuk (November 14–16, 2008), Bijli (April 14–16, 2009) and Aila (May 24–26, 2009).

Wind data for Gopalpur clearly demonstrate the prevalence of a strong seasonality in the annual wind pattern associated with reversing monsoons. From June to September, the southwest monsoon prevails and the predominant wind direction is southwesterly followed by southerly. The wind speed is relatively higher (>4 m/s) during 40 % of days, and a maximum wind speed of 8 m/s or more was observed during extreme events. During post-monsoon, the dominant wind direction is northerly followed by easterly with an average wind speed of 2.5 m/s. During December to February, northwesterly winds prevail and in March winds become more easterly. The transition months (March to May) are different from other seasons, and the wind speed is relatively higher, sometimes exceeding more than 8 m/s. The dominant wind direction is southerly followed by southwesterly.

3.1.1 Sea and land breeze

Sea and land breeze are generated by thermally induced local circulation found in the coastal regions and driven by differences in heating rates over land and the sea. The diurnal variation of sea and land breeze circulation is an essential aspect of the phenomenon, and the important characteristics are frequency of occurrence, intensity and duration, time of onset and cessations (Furberg et al. 2002). The wind data available at 10-min intervals for the period September 2008 to May 2009 are analyzed, and the sea and land breeze arrival and cessation are computed on monthly basis (Fig. 3).

At morning, the sea breeze gradually sets around 9–11 a.m. with the change in wind direction from NNW to SSE (Fig. 3). During September, the frequency of occurrence of sea-land breeze is minimum, and no particular trend exists. From October to January, the onset of sea breeze starts around 9 a.m. and completely changes from land to sea breeze in 2 h and continues till 7–8 p.m. The cessation of sea breeze and arrival of land breeze is very slow and takes roughly 4–5 h. The onset of sea breeze is comparatively early during February and March, i.e., around 8:30 a.m., with one-hour transition period changing from land to sea and remaining active for long time (12–14 h). During April and May, the frequency of occurrences of sea-land breeze is less than 20 %. The pre-monsoon and SW

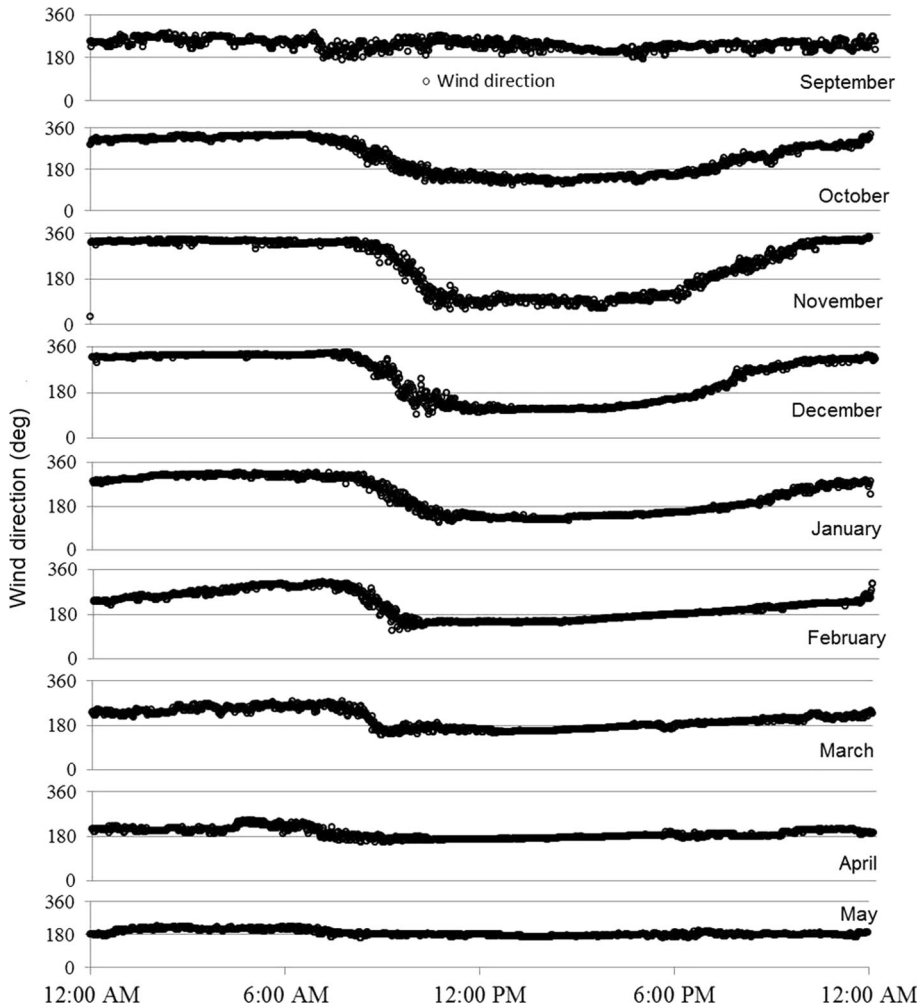


Fig. 3 Monthly averages of wind direction recorded at 10-min interval (except June, July and August)

monsoon, the wind is dominated by southerly and southwesterly, and thus, the frequency of occurrence of sea–land breeze is minimum.

3.1.2 Significant wave height

The significant wave height (H_s) for one-year period (2008–2009) ranged from 0.26 to 3.29 m with an average of 1.06 m, and the distribution is shown in Fig. 4a. During the southwest monsoon months (JJAS), H_s ranged from 0.7 to 3.29 m with an average of 1.49 m; post-monsoon (ON) values are from 0.4 to 2.18 m with a mean value of 0.88 m. Similarly, during the fair weather months (DJF), H_s ranged from 0.26 to 1.83 m with an average of 0.53 m, and pre-monsoon/transition months (MAM) recorded a range of 0.35–2.19 m with an average of 1.09 m.

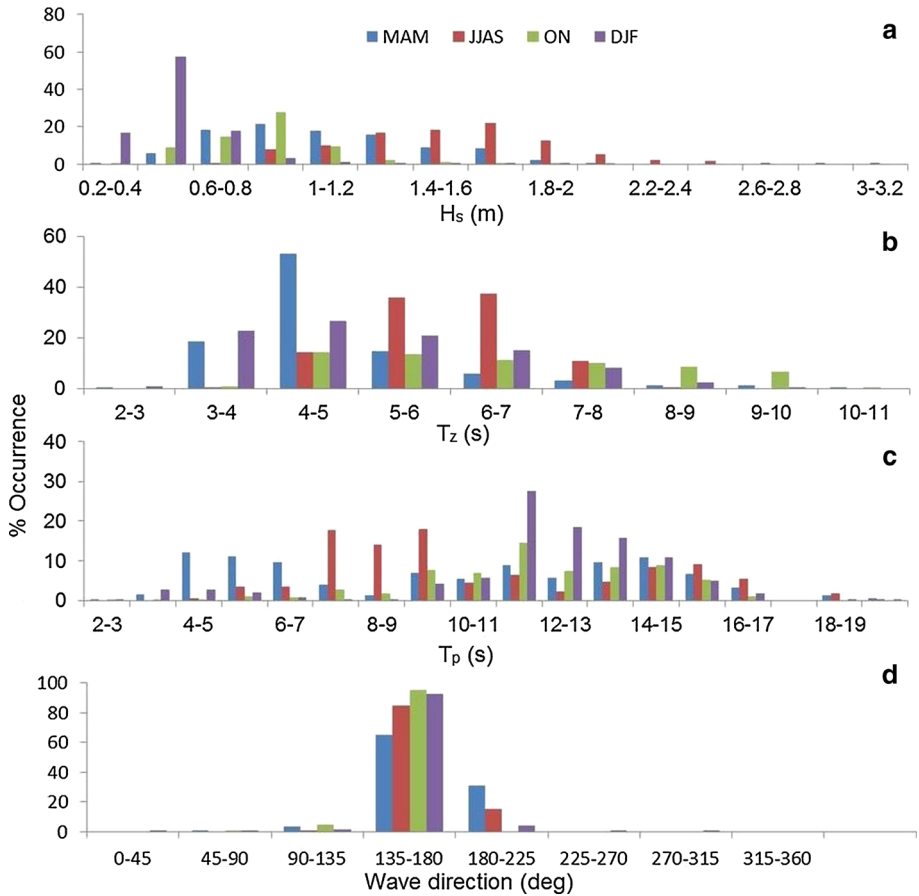


Fig. 4 Percentage occurrence, **a** significant wave height (H_s), **b** zero-crossing wave period (T_z), **c** peak wave period (T_p) and **d** direction (θ) for 2008–2009

The percentage distribution of significant wave height during pre-monsoon months shows that 50 % of waves are about 1–2 m high and the remaining 50 % are between 0.4 and 1.0 m. During SW monsoon, 80 % of waves are between 1.2 and 2 m and about 10 % of waves are between 2.2 and 3.4 m. During post-monsoon, 92 % of the waves are between 0.6 and 1.2 m and 41 % of the waves are 0.8–1 m. During the fair weather season, the wave intensity is less; about 94 % of waves are between 0.2 and 0.8 m. The maximum value of H_s exceeding 2 m was observed mostly during July and August due to consistent high wind conditions in the BoB during depressions. The maximum value of H_s less than 1 m was recorded mostly during December and January, and the lowest wave activity (0.26–0.71 m) occurred in December 2008.

3.1.3 Zero-crossing wave period

The distribution of zero-crossing periods (T_z) is shown in Fig. 4b. T_z has a wider range (2–14 s) during pre-monsoon (MAM) and narrow range (4–9 s) during SW monsoon.

Though during pre-monsoon the T_z varies over a wider range, nearly 87 % fall within 4–6 s. During monsoon, T_z in the range of 5–8 s contributes nearly 99 % of the distribution and 5–6 and 6–7 s group shares nearly 73 %. During post-monsoon (October to November), 87 % of T_z distribution is shared by 5–9 s. During fair weather months, 97 % of T_z falls between 4 and 8 s; 71 % are in a narrow range of 4–6 s.

3.1.4 Peak wave period

The peak wave period ranged from 2.2 to 20 s with an average of 11.16 s and standard deviation (SD) of 3.36 s. The distribution of peak wave period is presented in Fig. 4c. During SW monsoon, T_p ranged from 5 to 20 s and shows occurrence of two different wave groups. A narrow range of waves with peak wave period of 7–10 s contribute 50 % of the total distribution and 23 % of the distribution in the range of 14–17 s. The peak period distribution during post-monsoon mainly ranged between 9 and 15 s (81 %) and about 22 % falls in the range of 11–12 s. During fair weather period, T_p is distributed in a wider range (2–20 s), but a major percentage (74 %) is shared by 11–15 s. During transition months, T_p ranged from 3 to 20 s and almost uniformly distributed.

3.1.5 Mean wave direction

The time-series plot of mean wave direction is shown in Fig. 4d. Annually, the mean wave direction ranged in 72° and 280° with respect to north, with mean wave direction of 166° , and the variation is narrow, throughout the year. Seasonally, the ranges of wave direction in June to September, October to November, December to February and March to May are 82° to 211° , 80° to 210° , 90° to 180° and 76° to 280° with mean direction of 169° , 166° , 159° and 158° , respectively. SSE waves are dominant throughout the year and do not follow the conventional seasonal wind regime of southwest and northeast.

3.2 Sea and swell wave characteristics

The variation of wave heights (H_{sw} , H_{ss} , H_s), zero-crossing periods (T_{sw} , T_{ss} , T_z), mean wave directions (θ_{sw} , θ_{ss} , θ) and percentage of occurrence of sea and swell to H_s are plotted in Fig. 5a–d. Annually, 51.5 % of waves are dominant by sea and 48.5 % by swell; dominance of swell over sea is observed during October to January and March. Maximum swell dominance occurs during the month October (89.8 %), and maximum sea dominance is observed during April (86.3 %). On seasonal basis, sea waves dominate during JJAS (62.5 %) and MAM (70 %), whereas swells dominate during ON and DJF (77 and 63 %), respectively. The coast experiences predominate swell waves during post-monsoon and fair weather period, whereas seas are dominant during pre-monsoon and SW monsoon. However, an earlier study along the west coast (Aboobacker et al. 2011) reported dominance of swell (>90 %) during June to September and more than 75 % during October to December. In Cuddalore region, southeast coast of India, the seas and swells are dominated by 76 and 24 %, annually (Patra and Jena 2012). The contribution of swells to H_s is 63.2 % and that of seas is 36.8 % along Visakhapatnam coast during June to September (Suresh et al. 2010). Regression analysis between H_s and H_{sw} indicates a better correlation of 0.91 compared with 0.87 H_s and H_{ss} . The wave height due to the locally generated seas from

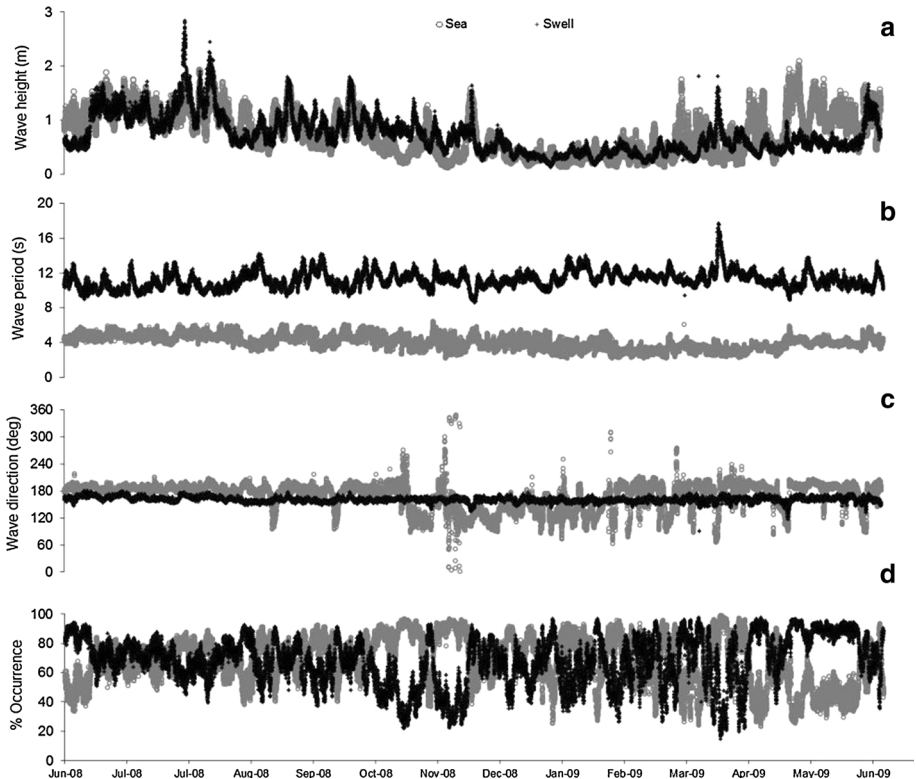


Fig. 5 Time-series plots of sea and swell, **a** wave height, **b** period, **c** direction and **d** percentage occurrence

different directions contributes more in H_s , which confirms that the estimated magnitude of H_s is mainly contributed by seas than by swell waves.

The wave period (T_z) ranges from 2.6 to 13.8 s, with an average of 5.7 s and mean T_{sw} and T_{ss} of 4.1 and 11.2 s, respectively. Measured T_z is uniformly distributed: 3–5 s for T_{sw} , 4–7 s for T_z and 9–12 s for T_{ss} (Fig. 5b).

There is a distinct shift in sea wave direction between mid-November to mid-February and rest of the year. The mean sea wave direction during June to mid-November is 181° (southerly); mid-November to mid-February is 134° (south-easterly); and mid-February to end of May is 174° (Southerly). The change in sea wave direction on the transition day (between 15 and 16 November) is exactly 90° , and there is an average shift of 45° between mid-November and mid-February. The predominant swell direction throughout the year is 160° (SSE). Directional spreading of swell waves is very less ($<6^\circ$), due to the predominant SSE swells that are prevalent throughout the year. However, the spreading of sea waves is higher ($>30^\circ$). The observed higher directional spreading of sea waves and spectral width reduces the spectral energy and resulted multi-peaked and multi-directional wave spectrum. However, the major effect of directional spreading affects only on direction of the wave spectra without affecting amplitude of the sea waves (Elgar et al. 1993). Hence, the shape of directional spectra of swell wave has only small effect on the magnitude of the total wave energy spectrum.

3.2.1 Hourly variation of sea, swell and significant wave height

The hourly variations of H_{sw} , H_{ss} and H_s for the period June 2008 to May 2009 are shown in Fig. 6. Usually, the H_{sw} starts gaining height at 9 a.m. in congruent with onset of sea breeze and continues till afternoon. The wave height attains its peak around 2 PM and gradually decreases as land breeze sets in. The average magnitude of H_{sw} and H_{ss} is similar during July and August. However, in June there is a 20 % increase in H_{sw} compared with H_{ss} . In September and October, H_{sw} and H_{ss} follow the similar pattern; H_{sw} attains its maximum magnitude at noon and then decreases gradually. During November, H_{ss} is found to be double the magnitude of H_{sw} , which is mostly contributed by long swells from far-off places. In December, an increase of 20 % in H_{ss} is noticed compared with H_{sw} . During January and February, the trend of H_{sw} is same as that of JJAS. The magnitude of H_{sw} increases compared with H_{ss} between March and May. The increase in H_{sw} is about 40 % during 9 a.m. to 6 p.m. in March and April, and the mean H_{sw} is twice that of H_{ss} during May.

3.3 Wave spectral analysis

Wave spectra are analyzed at every 3-h interval, and the percentage occurrence of single-, double- and multi-peaked spectra is presented in Fig. 7. On an annual basis, the maximum spectral energy density (E_{max}) varied between 0.04 and 30.64 m^2/Hz with an average value of 1.48 m^2/Hz (Table 1). Earlier, Mishra et al. (2011) reported that the single-peaked spectrum occurs during extreme events with peak period of 10–12 s and double- and multi-peaked spectrum during lower sea state. High wave energy is observed during the period of SW monsoon and extreme events (cyclones and low pressures), and it generally occurs in the low-frequency region (0.1–0.15 Hz). Regression analysis for the present set of data considered in the study shows a correlation coefficient of 0.75 between H_s and observed E_{max} compared with 0.82 reported earlier for east coast of India (Kumar et al. 2004).

Throughout the year, percentage occurrence of single-, double- and multi-peaked spectra is 22, 40 and 38 %, respectively. During June and July, the double-peaked spectra (45.4, 50 %) dominate over the multi-peaked spectra (40.4, 37.5 %), whereas in August and September multi-peaked (50.8, 44.6 %) spectra dominate double-peaked spectra (34, 40.4 %). During SW monsoon, the occurrence of single-peaked spectra is less than 15 % which corresponds to the period of low-pressure systems over BoB. During October to January and March, the contribution of each observed spectrum is relatively same (30 to 40 %). However, the double-peaked spectra dominate (50 %) in February, followed by single-peaked and multi-peaked spectra. During April and May, multi-peaked spectra are dominant (43.8, 55.2 %), followed by double-peaked (40.8, 36.7 %) spectra. Highest percentages of single-, double- and multi-peaked spectra are observed during November (33 %), February and July (50 %), and May (55.2 %), respectively.

The monthly average of wave spectrum was calculated between frequencies 0.025–0.58 Hz measured at 30-min intervals to discern the wave spectral characteristics on seasonal basis (Fig. 8). During SW monsoon, the spectral energy density peaks are formed at two sets of narrow-band frequencies for the months of June and July; however, the peak of sea wave is more flat in shape and a wider range in frequency for August and September. This leads to formation of double-peaked spectra during June and July months and multi-peaked spectra in August and September. The magnitudes of spectral energy density of sea wave are dominated during June, July and August and swells in September. The resultant spectra of October and November are single peaked and swell dominated. The wave

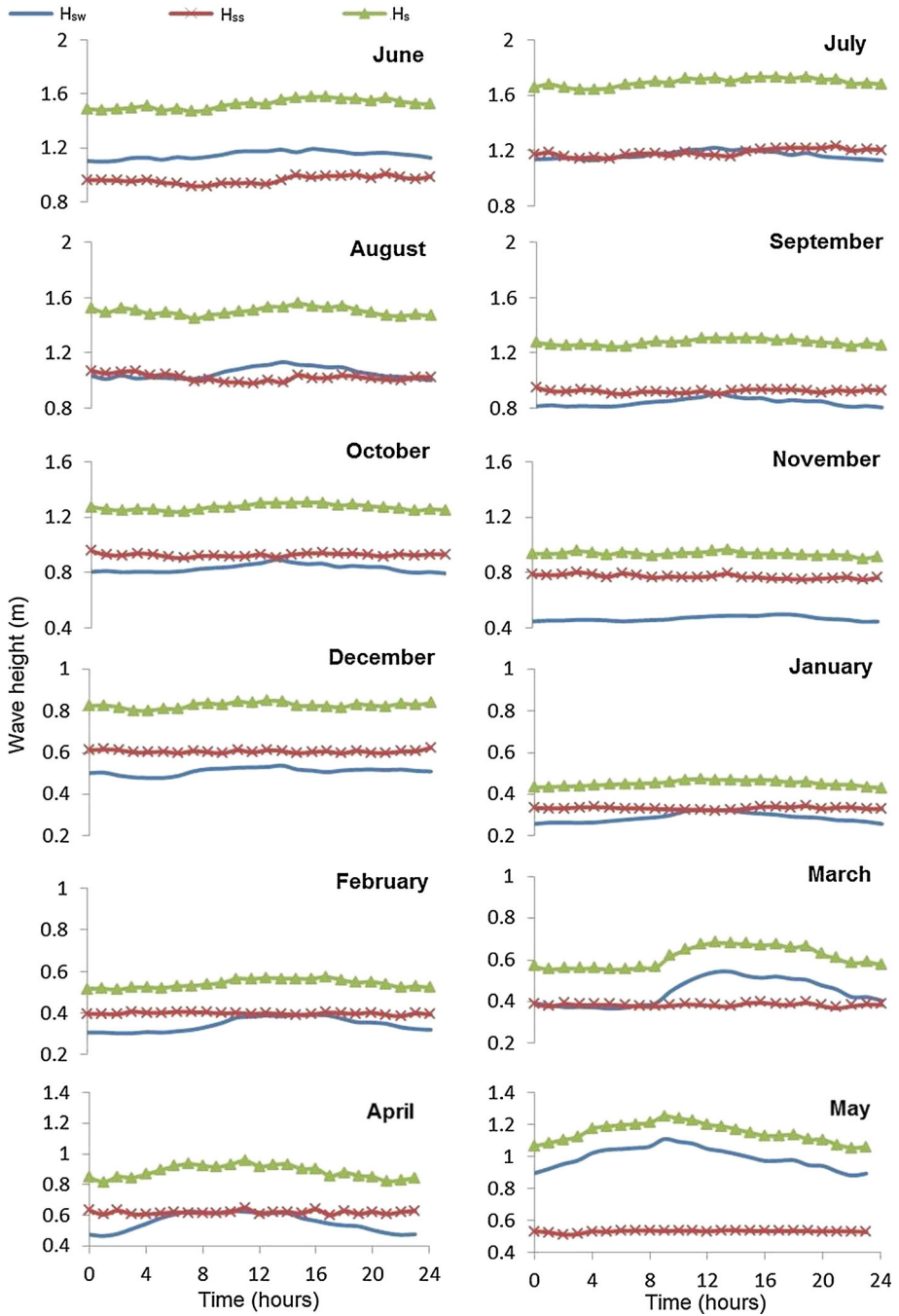


Fig. 6 Hourly variation of sea wave height (H_{sw}), swell wave height (H_{ss}) and significant wave height (H_s) for the period June 2008 to May 2009

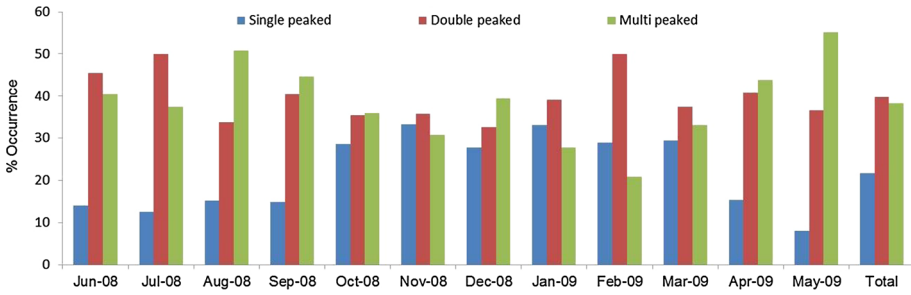


Fig. 7 Percentage occurrence of single-, double- and multi-peaked wave spectra for 2008–2009

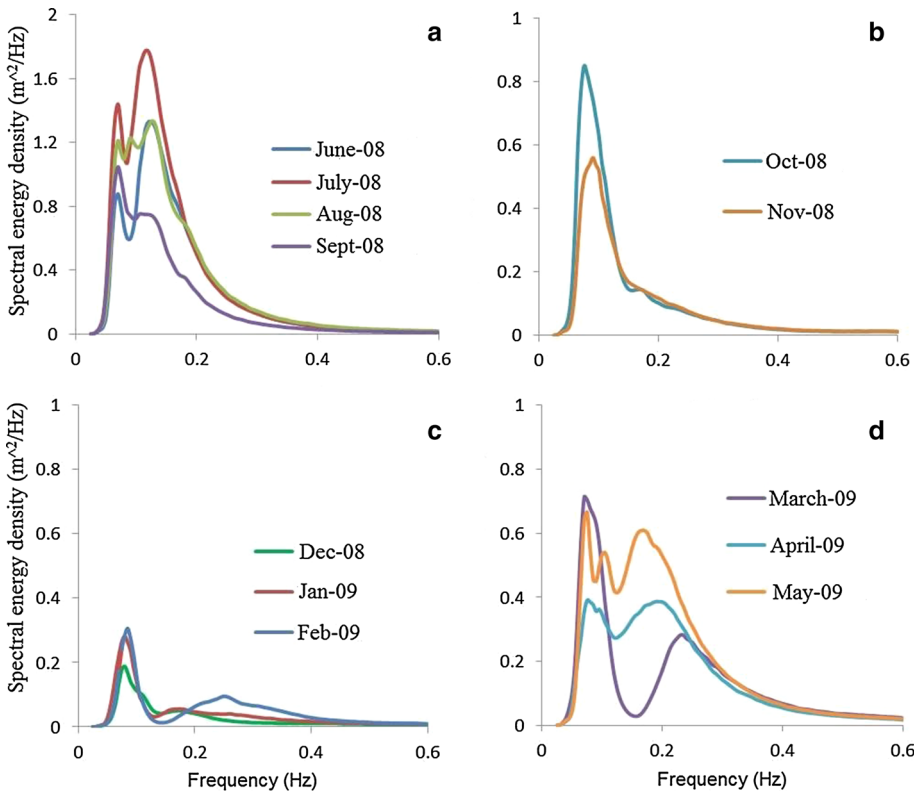


Fig. 8 Monthly averages of spectral energy density, **a** JJAS, **b** ON, **c** DJF and **d** MAM for 2008–2009

spectra of December, January and February are dominated by swell waves, and there is no particular peak of sea wave spectrum. The energy of sea wave spectrum is very low during these months. The resultant wave spectrum during March has two distinct peaks in the both sea and swell wave regimes, whereas during April and May, sea wave has more than two peaks with broader range of frequencies.

Spectral peakedness parameter (Q_p) known as Goda’s peakedness parameter is a measure of the irregularity of the sea state (Goda 1970). Theoretically, Q_p becomes very

large for narrow-band spectra and remains low for broad-band spectra, and under normal conditions, it remains within 1.5–5. In the present study, Q_p varied between 1 and 8.5 with an average of 1.84 and SD of 0.66. Majority of the wave spectra are broader, and Q_p value falls within the range of 1.2–2.5. Usually, spectral width (ε) and narrowness (ν) parameters vary from 0 to 1 and have smaller values for narrower spectra and larger for broader spectra. The spectral width (ε) parameter for 1 year ranged from 0.53 to 0.96 with a mean 0.8 and SD of 0.07; a major portion falls in the range of 0.7–0.85. The higher magnitude of spectral width parameter indicates the presence of sea waves accompanying the swell waves during most of the period. The spectral narrowness (ν) parameter varies between 0.33 and 1 with a mean of 0.59 and SD of 0.13. The predominant values for SW monsoon fall in the range of 0.5–0.6, contributing to 48 % of the total distribution, and 0.4–0.6 range occupies 85 % of the distribution. During post-monsoon, 0.5–0.7 range occupies nearly 55 % of the total distribution. In fair weather, the dominant distribution is in the range of 0.6–0.7, and for pre-monsoon, the highest percentage is within 0.4–0.5.

3.4 Long-term wave characteristics off Gopalpur

The wave records for the western BoB reported in the literature are summarized in Table 2 for comparison. Based on ship observed data, the wave directions ranged between 30° and 90°, 180° and 240°, and 180° and 210° for the pre-, SW and post-monsoon seasons, respectively, and H_s varied between 0.2 and 2.4 m (Chandramohan and Nayak 1994). In the present study, wave data of three different years (1994, 2008–2009 and 2013–2014) have been compiled and the monthly averages of H_s , T_p , T_z and θ are presented (Fig. 9). The standard deviations for all the wave parameters for the three different years considered are less than 10 % and quite comparable. Monthly mean H_s is higher (>1.5 m) during SW monsoon (JJAS) and lower (<0.6 m) during post-monsoon period (DJF). The wave period T_z is higher (>7 s) during post-monsoon (ON) and lower (<5 s) during pre-monsoon (MAM) periods. The mean wave direction (mode of monthly mean) is southerly during JJAS and SSE for the rest of the year.

The seasonal wave rose diagrams for significant wave height for the years 1994, 2008–2009 and 2013–2014 are presented in Fig. 10. During SW monsoon, waves are dominantly from SSW, S and SSE. However, the percentage occurrence in magnitude is differently attributed to prevailing local wind regime. SSE waves dominate during October and November, controlled by the frequency and magnitude of tropical cyclones formed over southeastern BoB. The months of DJF are calm ($H_s < 0.5$ m), i.e., 48 % in 1994, 50 % in 2008–2009 and 33 % in 2013–2014 and mostly from SSE. However, the waves from E, SE and ESE are recorded with lesser frequency compared with S and SSE waves. The MAM are dominated by SSW, S and SSE waves. Though it was discussed earlier, with the onset of SW monsoon during this transition, the SSW wind initiates SSW waves.

The orientation of the coastline and the local bathymetry of the area modify the wave incidence angle to a large extent (Coastal Engineering Manual 2008). In case of Gopalpur, the bathymetry is steep from 3 to 10 m depth and becomes fairly smooth and gentle further seawards and the isobaths run shore parallel (Rao et al. 1989). As a result, waves approaching from SSW and E become S and ESE, whereas waves from the SE continue to move in the same direction without any significant refraction in the shallow region (Mishra et al. 2001).

Extreme value analysis is usually done to design the structures along coastal fronts. It is a statistical parameter that estimates the possibility of a wave greater than 100 years return value, or even of several such waves, occurring within a few years. The wave height

Table 2 Summary of wave characteristics along western Bay of Bengal

Sl. no	Location (lat./long.) and deployment depth	Measurement period	Observations	References
1	Paradip 20 8.5'N 86 44.67E 30 m	May 1996–January 1997	Pre-monsoon: wave height (H_s)—0.9–2.7 m and wave direction (θ)—SSW to SSE SW monsoon: max. H_s —4.2 m and θ —S to SSE NE monsoon: max. H_s —2.1 m and θ —S to SSE	Aboobacker et al. (2009)
2	Gopalpur 10 m 15 m 23 m	Ship-based data 1995–1996 2008–2009	Pre-monsoon: H_s —0.2 to 2.2 m and θ —30° to 90° SW Monsoon: H_s —0.5 to 2.2 m and θ —180° to 240° NE monsoon: H_s —0.2 to 2.4 m and θ —180° to 210° Yearly H_s range: 0.2–2.5 m Yearly H_s range: 0.2–3.3 m Pre-monsoon: H_s —0.35 to 2.19 m (mean 1.09 m) and θ —76° to 280° (mean 158°) SW monsoon: H_s —0.7 to 3.29 m (mean 1.49 m) and θ —82° to 211° (mean: 169°) NE Monsoon (ON): H_s —0.4–2.18 m (mean 0.88 m) and θ —80° to 210° (mean: 166°) Post-monsoon (DJF): H_s —0.26 to 1.83 m (mean 0.53 m) and θ —90° to 180° (mean: 159°)	Chandramohan and Nayak (1994) Kumar et al. (2006) Present study
3	Tikkavanipalem (Vishakhapatnam) 12 m	December 1997–November 1998	Yearly H_{sw} —0.2 to 1.7 m (mean: 0.7 m) Yearly θ_{sw} —92° to 213° (mean: 162°) Yearly H_{ss} —0.1 to 1.8 m (mean: 0.6 m), Yearly θ_{ss} —104°–201° (mean: 159°)	Kumar et al. (2001)
4	Gangavaram 17 38.011N 83 15.946E 20 m	June–September 2009	SW monsoon: H_s —0.88 to 2.62 m (mean: 1.61 m), H_{max} —1.05 to 5.1 m (mean: 2.45 m) and θ —120.9° to 192.7° (mean: 159.6°)	Suresh et al. (2010)
5	Puduchery 11 55'26"N 79 51'03"E 10 m	2009–2011	Pre-monsoon: θ —E to SSE SW monsoon: θ —ENE to SSE NE monsoon: θ —E to ENE Yearly max. H_s —6 m and H_{max} —8 m	Glejin et al. (2013)

Table 2 continued

Sl. no	Location (lat./long.) and deployment depth	Measurement period	Observations	References
6	Cuddalore 30 m	January 2010– January 2011	Pre-monsoon: H_s —0.24 to 1.88 m (mean: 0.65 m) and θ —ESE to SE (129°) SW monsoon: H_s —0.15 to 1.62 m (mean: 0.76 m) and θ —SE to SSE (134°) NE monsoon: H_s —0.25 to 2.78 m (mean: 1.01 m) and θ —ENE to ESE (mean: 99°), Pre-monsoon: H_s —0.5 to 1 m and θ —60° to 120°, SW monsoon: H_s —0.5 to 1 m and θ —90° to 120°, NE monsoon: H_s —0.5 to 1.5 m and θ —30° to 120° Yearly mean H_s —0.67 and θ —98	Patra and Jena (2012)
7	Nagapattinam 10 m	March 1998– February 1999	Yearly mean H_s —0.67 and θ —98	Kumar et al. (2002)
8	Pamban Bay 9 19.16°N 79 26.02°E 12 m	February 2010– March 2011	Yearly H_s —0 to 1.8 m, (mean: 0.5 m) and H_{max} : 0–3.6 m. November to March: θ —N to NE and February to October: θ —NE to SE	Gowthaman et al. (2013)
9	Gulf of Munnar 9 6.75°N 79 24.42°E 12 m	February 2010– March 2011	Yearly H_s —0.2 to 2.7 m (mean: 0.9 m), H_{max} —0.3 to 5.4 m (mean: 1.4 m) Pre-monsoon: θ —90° to 200° SW monsoon: θ —140° to 230° NE monsoon: θ —85° to 150°	Gowthaman et al. (2013)
10	Kannirajapuram (GOM) 12 m	March 1997– February 1998	Pre-monsoon: H_s —0.33 to 1.97 m, H_{max} —0.44 to 2.81 m and θ —81° to 201° SW monsoon: H_s —0.59 to 1.87 m, H_{max} —0.87 to 2.96 and θ —92° to 245° NE monsoon: H_s —0.35 to 1.23 m, H_{max} —0.45–1.79 m and θ —2° to 357°	Kumar et al. (2000)

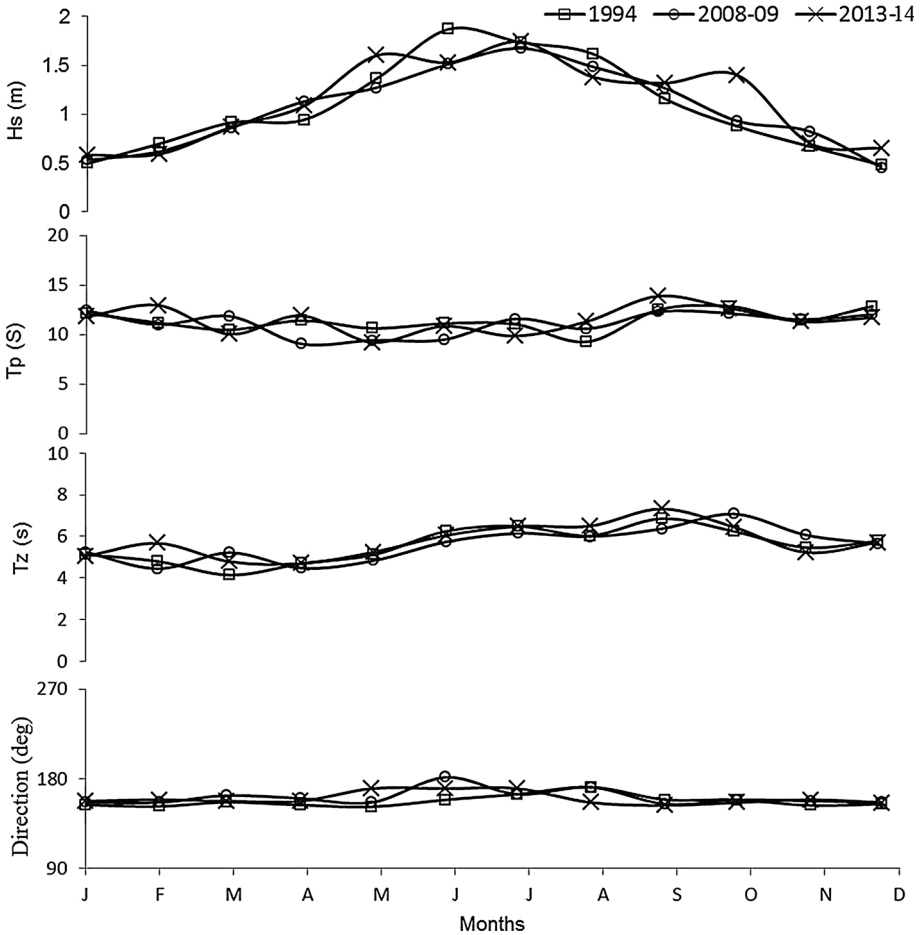


Fig. 9 Monthly averages plot of significant wave height (H_s), zero-crossing wave period (T_z), peak wave period (T_p) and direction (θ) off Gopalpur for 1994, 2008–2009 and 2013–2014

specified for the return value can be either H_s , or H_{max} or even the height of an individual wave. The return period for a range of 1–100 years is calculated using 3 years of observed wave data. A return period of 1 in 1 means from a given dataset this event will ensue once in a year. So, at Gopalpur significant wave height of 7.1, 7.4 and 7.8 m can occur once in 10, 50 and 100 years of cycle, respectively. The choice of distribution to fit the data depends on the type of distribution and application.

3.5 Cyclone wave characteristics off Gopalpur

The cyclone wave characteristics associated with wind and surge parameters are given in Table 3. The maximum and significant wave height for September 2008 deep depression was 3.8 and 2.4 m, respectively, with predominant wave directions of S and SSE. During the cyclone events for Rashmi, H_{max} and H_s were 2.6 and 1.45 m, respectively (predominantly SSE); for Khaimuk, H_{max} and H_s were 3.6 and 2.2 m with predominant wave

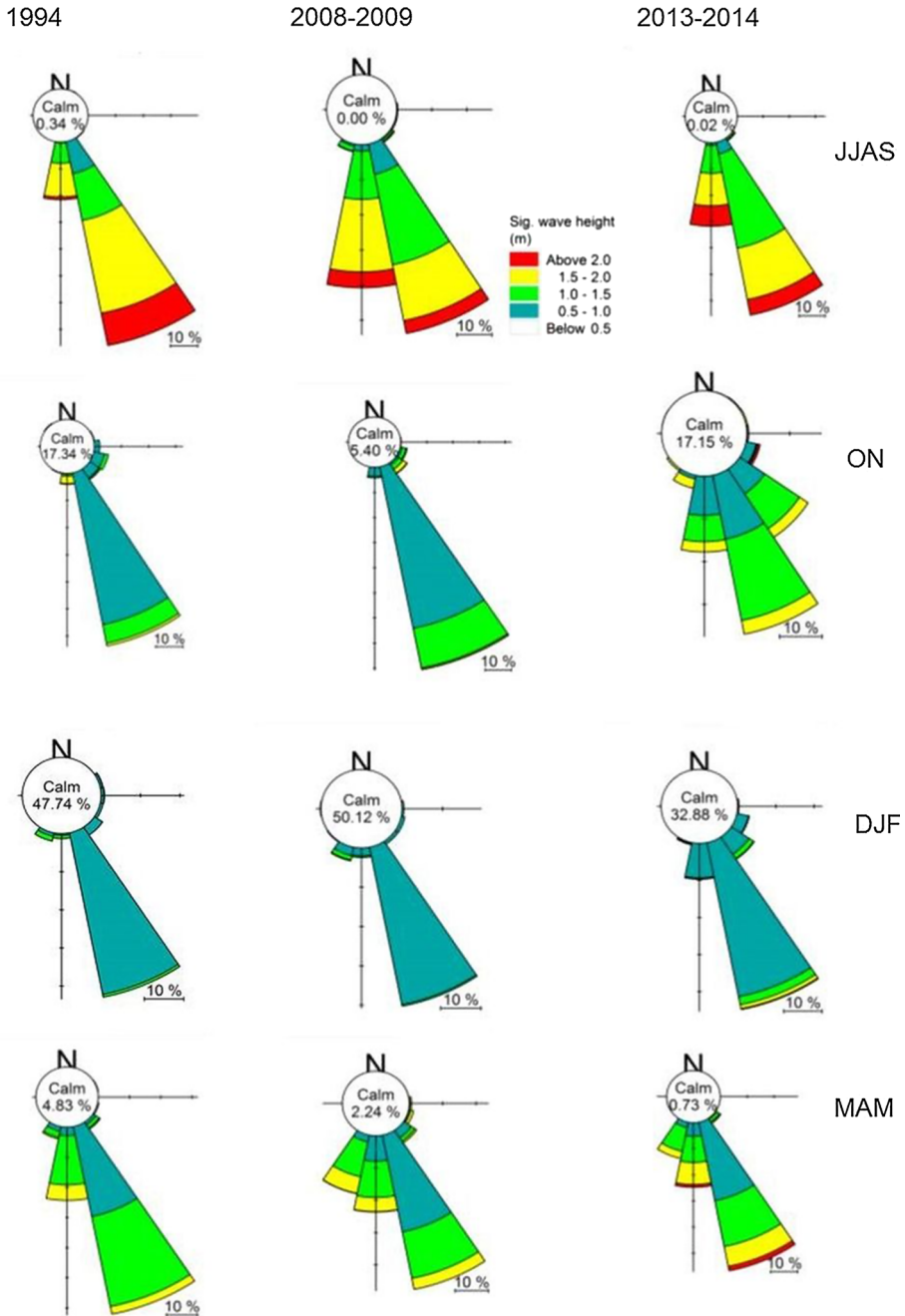


Fig. 10 Wave rose diagrams for JJAS, ON, DJF and MAM for 1994, 2008–2009 and 2013–2014

direction of SE; for Bijli, the H_{max} and H_s were 3.5 and 2.1 m with predominant directions of S and SSW; for Aila, the H_{max} and H_s were 3.2 and 2.07 m with predominant direction of SSE, followed by S. The H_{max} and H_s observed during very severe cyclonic storm

Table 3 List of cyclone systems between June 2009 and very severe cyclonic storm Phailin (October 2013) and their associated atmospheric, wave and surge parameters

Type of weather disturbances	Duration	Maximum sustained wind speed (m/s)	Maximum pressure drop and lowest pressure recorded (hPa)	Maximum significant wave height (m)	Predicted wave height from model (m)	Sea level during storm (m)	Remarks
Low pressure	July 29, to August 9, 2008	8.5	14 (990)	3.27	3.09	0.41	Land depression at Gopalpur (Mishra et al. 2011)
Deep depression	September 15–19, 2008	15.4	15.3 (991)	2.43	2.32	0.22	Land depression crossed near Chandipur (400 km north of Gopalpur)
Cyclone Rashmi	October 25–27, 2008	23	14 (998)	1.45	1.25	0.36	The cyclone crossed 500 km away from Gopalpur and hit Bangladesh coast
Cyclone Khaumic	November 13–16, 2008	20.6	9.8 (994)	2.2	2.13	0.18	The cyclone made landfall in the south Andhra Pradesh coast
Cyclone Bijli	April 14–17, 2009	20.6	8 (996)	2.1	1.73	0.12	The cyclone crossed parallel about 500 km away from Gopalpur and hit Chittagong, Bangladesh coast
Cyclone Aila	May 23–26, 2009	31	29 (968)	2.07	1.48	0.39	The cyclone hit near Sagar Island, West Bengal coast
VSCS Phailin	October 9–13, 2013	59.2	66 (940)	6.84	6.95	1.5	Landfall at Gopalpur (Murty et al. 2014)

(VSCS) Phailin (October 12, 2013) at Gopalpur were 13.5 and 6.84 m, respectively (Amrutha et al. 2014).

Maximum loss of life and property were recorded during October 1999 Orissa super cyclone due to inundation (surge height of 7.95 m) near Paradeep (Kalsi 2006), followed by VSCS Phailin (surge height of 1.5 m) that hit near Gopalpur coast. However, during the period June 2008 to May 2009, the observed highest surge of 0.41 m was recorded at Gopalpur associated with August 2008 depression. During other storm events of 2008–2009, the surge heights were 0.22 m for September 2008 depression, 0.36 m for cyclone Rashmi, 0.18 m for cyclone Khaumic, 0.12 m for cyclone Bijli and 0.39 m for cyclone Aila. During all cyclones, no loss of life and property were reported other than coastal erosion to some extent.

3.6 Wave modeling

MIKE 21 spectral wave model simulated for the period June 2008 to May 2009 for different wave parameters is validated with the measured values, and the comparisons of wave height (H_s), wave period (T_z) and wave direction (θ) are shown in Fig. 11. The estimates of statistical wave parameters between measured and simulated are given in Table 4. The correlation coefficient between measured and simulated H_s , T_z and θ is 0.85, 0.55 and 0.49, respectively, and simulated wave heights reasonably agree with our observations. Model simulated H_s , T_z and θ have bias of 0.05 m, 0.27 s and -5.69° and RMS errors of 0.1 m, 0.44 s and 9.19° , respectively. The simulated wave directions follow the pattern of the observed sea wave direction for the entire year. However, the model

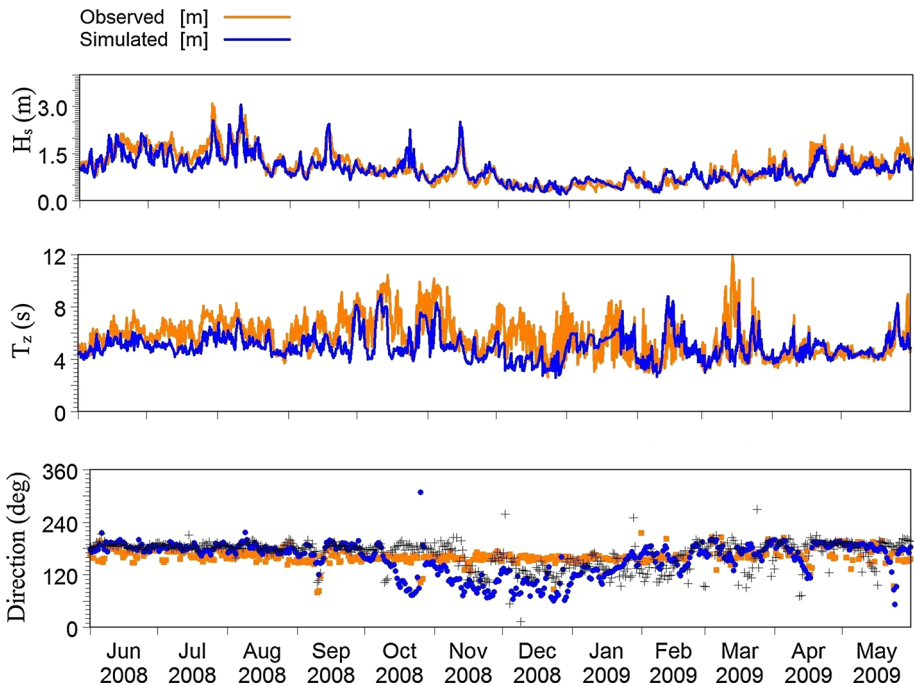


Fig. 11 Comparison between observed and simulated significant wave height (H_s), zero-crossing wave period (T_z) and wave direction (sea wave direction is indicated as *plus sign*)

Table 4 Statistics of measured and simulated wave parameter

Statistics	Significant wave height (H_s)	Wave period (T_z)	Wave direction (θ)
Correlation coefficient	0.86	0.55	0.49
RMS error	0.10 m	0.44 s	9.19°
Bias	0.05 m	0.27 s	-5.69°

wave direction for the period October to February does not coincide with the observed as the swell direction approaching from SSE dominates, nullifying the wind-generated seas. The long-term data for three different years also indicate the absence of wave approaching from northeast direction. The disagreement between measured and simulated wave directions emphasizes the importance of nearshore wave observations which could be utilized for sediment transport computation and other coastal zone management practices along east coast of India.

4 Conclusion

Understanding of nearshore wave characteristics is crucial for beach erosion/deposition processes, sediment transport, design of coastal structures and in general management of coastline. Wave climate off Gopalpur is studied for three different years spanning over two decades, indicating that monthly and seasonal wave parameters vary within a range and repetitive. The single-, double- and multi-peaked wave spectra percentage during a year are 22, 40 and 38, respectively. The ‘seas’ dominate during pre- and SW monsoon, whereas ‘swells’ dominate during rest of the year. On the basis of significant wave height and energy distribution, the wave climate could be grouped into four categories, *i.e.*, high wave energy during June to September (mean H_s : 1.49 m and E_{max} : 2.56 m²/Hz); low energy during October and November (mean H_s : 0.88 m and E_{max} : 1.26 m²/Hz); very low in the month of December, January and February (mean H_s : 0.53 m and E_{max} : 0.40 m²/Hz); and moderate energy during March to May (mean H_s : 1.09 m and E_{max} : 1.24 m²/Hz). As a result, the coast experiences erosion during March to September and accretion during October to February (Mishra et al. 2001; Mohanty et al. 2012). The predominant swell wave direction is SSE throughout the year. Though the sea wave direction changes to easterly during mid-November commensurating with wind pattern over Indian subcontinent and north Indian Ocean, the swells from SSE dominate the seas that drive unidirectional longshore sediment transport toward north along this coast (Mishra et al. 2014). This phenomenon is ubiquitous along the east coast of India; the southern side of the ports and coastal structures is wide and depositional and the northern coast is narrow and erosional (Kumar et al. 2006; Ranga Rao et al. 2009; Mohanty et al. 2012). The low-pressure system during August 2008 caused sea level rise of 0.41 m, as a result of which episodic erosion events occurred all along the coast (Mishra et al. 2011).

The simulated and measured wave heights are in good agreement, while the direction during November to February varies, due to dominance of SSE swell approaching from Indian Ocean. Further, the long-term distribution of waves is important to predict the highest possible waves and their probable return periods. The estimated significant wave height of 7.1, 7.4 and 7.8 m could occur in 10, 50 and 100 years of cycle, respectively. Therefore, for any coastal developmental activities along east coast of India, the wave data need to be critically examined and utilized.

Acknowledgments The present study is a part of the Ph.D. thesis of the first author. The data were collected by ESSO-ICMAM, Chennai, NIO, Goa, and ESSO-INCOIS, Hyderabad, under different R&D programs, duly acknowledged. We are grateful to Secretary, Ministry of Earth Sciences, Government of India, New Delhi, Project Director, ICMAM, Chennai, and Berhampur University, Odisha, for their supports and encouragement. The help rendered by IMD, Gopalpur, and Gopalpur Port Limited is acknowledged. We thank the anonymous reviewers for their valuable suggestions.

References

- Aboobacker VM, Vethamony P, Sudheesh K, Rupali SP (2009) Spectral characteristics of the nearshore waves off Paradip, India during monsoon and extreme events. *Nat Hazards* 49:311–323
- Aboobacker VM, Vethamony P, Rashmi R (2011) “Shamal” swells in the Arabian Sea and their influence along the west coast of India. *Geophys Res Lett* 38:1–7
- Alam M, Hossain A, Shafee S (2003) Frequency of Bay of Bengal tropical storms and depressions crossing different coastal zones. *Int J Climatol* 23:1119–1125
- Amrutha MM, Kumar VS, Anoop TR, Balakrishnan Nair TM, Nherakkol A, Jayekumar C (2014) Waves off Gopalpur, northern Bay of Bengal during Cyclone Phailin. *Ann Geophys* 32:1073–1083
- Balaguru K, Taraphdar S, Leung LR, Foltz RR (2014) Increase in the intensity of post monsoon Bay of Bengal tropical cyclones. *Geophys Res Lett* 41(10):3594–3601
- Chandramohan P, Nayak BU (1994) A study for the improvement of the Chilika lake tidal inlet, east coast of India. *J Coast Res* 10(4):909–918
- Chandramohan P, Nayak BU, Raju VS (1988) Application of longshore transport equations to the Andhra coast, east coast of India. *Coast Eng* 12:285–297
- Chauhan OS (1995) Monsoon-induced temporal changes in beach morphology and associated sediment dynamics, central east coast of India. *J Coast Res* 11(3):776–787
- Coastal Engineering Manual (2008) U.S. Army coastal engineering research centre, Department of the Army, Corps of Engineers, Washington, DC
- Datawell BV (2006) Wave Rider Reference Manual, Datawell BV, Zumerlustra 4, 2012 LM Haarlem, The Netherlands
- DHI (Danish Hydraulics Institute) (2011) DHI Software, DHI Water and Environment, Agern Alle 5, DK-2970. Harshoalm, Denmark
- Elgar S, Guza RT, Freilich MH (1993) Observations of nonlinear interactions in directionally spread shoaling surface gravity waves. *J Geophys Res* 98(C11):299–305
- Furberg M, Stern DG, Baldi M (2002) The climatology of sea breezes on Sardinia. *Int J Clim* 22:912–932
- Gilhousen DB, Hervey R (2001) Improved estimates of swell from moored buoys. In: Proceedings of the fourth international symposium WAVES 2001, ASCE: Alexandria, VA, pp 387–393
- Glejin J, Kumar VS, Balakrishnan Nair TM (2013) Monsoon and cyclone induced wave climate over the near shore waters off Puducherry, south western Bay of Bengal. *Ocean Eng* 72:277–286
- Goda I (1970) A synthesis of breaker indices. *Jpn Soc Civ Eng* 2(2):227–230
- Gowthaman R, Kumar VS, Dwarakish GS, Mohan SS, Singh Jai, Ashok Kumar K (2013) Waves in Gulf of Mannar and Palk Bay around Dhanushkodi, Tamil Nadu, India. *Curr Sci* 104(10):1431–1435
- Hanson JL, Phillips OM (1999) Wind sea growth and dissipation in the open ocean. *J Phys Oceanogr* 29:1633–1648
- Islam T, Peterson RE (2009) Climatology of land falling tropical cyclones in Bangladesh 1877–2003. *Nat Hazards* 48(1):115–135
- Kalsi SR (2006) Orissa super cyclone: a synopsis. *Mausam* 57:1–20
- Komen GJ, Cavaleri L, Donelan M, Hasselmann K, Hasselmann S, Janssen PAEM (1996) Dynamics and modelling of ocean waves. Cambridge University Press, New York 532
- Kumar VS, Chandramohan P, Ashok Kumar K, Gowthaman R, Pednekar PS (2000) Longshore currents and sediment transport along Kannirajapuram coast, Tamil Nadu, India. *J Coast Res* 16(2):247–254
- Kumar VS, Ashok Kumar K, Raju NSN (2001) Nearshore processes along Tikkavanipalem Beach, Visakhapatnam, India. *J Coast Res* 17:271–279
- Kumar VS, Anand NM, Gowthaman R (2002) Variations in nearshore processes along Nagapattinam coast, India. *Curr Sci* 82(11):1381–1389
- Kumar VS, Anand NM, Kumar KA, Mandal S (2003) Multi-peakedness and groupiness of shallow water waves along Indian coast. *J Coast Res* 19:1052–1065
- Kumar VS, Ashok Kumar K, Raju NSN (2004) Wave characteristics off Visakhapatnam coast during cyclone. *Curr Sci* 86:1524–1529

- Kumar VS, Pathak KC, Pednekar P, Raju NSN, Gowthaman R (2006) Coastal processes along Indian coastline. *Curr Sci* 91:530–536
- Kumar VS, Ashok Kumar K, Pednekar P (2008) Observation on oceanographic parameters of nearshore waters off Yanam, during cyclonic storm. *Curr Sci* 94:1503–1508
- Kumar VS, Shanas PR, Dubhashi KK (2014) Shallow water wave spectral characteristics along the eastern Arabian Sea. *Nat Hazards* 70:377–394
- Mephaden MJ, Foltz GR, Lee T, Murty V, Ravichandran M, Vechhi GA, Vialard J, Wiggert JD, Yu L (2009) Ocean–Atmospheric interactions during cyclone Nargis. *EOS Trans AGU* 90(7):53–54
- Mishra P, Mohanty PK, Murty ASN, Sugimoto T (2001) Beach Profile studies near an artificial open-coast port along South Orissa, East Coast of India. *J Coast Res* 34:164–171
- Mishra P, Patra SK, Ramana Murthy MV, Mohanty PK, Panda US (2011) Interaction of monsoonal wave, current and tide near Gopalpur, east coast of India and their impact on beach profile; a case study. *Nat Hazards* 59(2):1145–1159
- Mishra P, Pradhan UK, Panda US, Patra SK, Ramana Murthy MV, Mohanty PK (2014) Field measurements and numerical modelling of nearshore processes at an open coast port on the east coast of India. *Indian J Mar Sci* 43(7):1277–1285
- Mohanty PK, Patra SK, Bramha S, Seth B, Pradhan UK, Behera B, Mishra P, Panda US (2012) Impact of Groins on beachmorphology: a case study near Gopalpur Port, East Coast of India. *J Coast Res* 28:132–142
- Mohapatra M, Mohanty UC (2004) Some characteristics of low pressure systems and summer monsoon rainfall over Orissa. *Curr Sci* 87:1245–1255
- Murty PLN, Sandhya KG, Bhaskaran PK, Jose Felix, Gayathri R, Balakrishnan Nair TM, Srinivasa Kumar T, Shenoi SSC (2014) A coupled hydrodynamic modeling system for PHAILIN cyclone in the Bay of Bengal. *Coast Eng* 93:71–81
- NCEP (National Centers for Environmental Prediction) (2009) NCEP blended ocean winds datasets for the year 2009. <http://dss.ucar.edu/datasets>
- Patra SK and Jena BK (2012) Sea and swell off Cuddalore, East coast of India. In: Proceedings of the 11th biennial of pan ocean remote sensing conference (PORSEC), Kochi, India
- Ranga Rao V, Ramana Murthy MV, Bhat Manjunath, Reddy NT (2009) Littoral sediment transport and shoreline changes along Ennore on the southeast coast of India: field observations and numerical modelling. *Geomorphology* 112:158–166
- Rao KM, Rajamanickam GV, Rao TCS (1989) Holocene marine transgression as interpreted from bathymetry and sand grain size parameters off Gopalpur, east coast of India. *Proc Indian Acad Sci* 98:173–181
- Rao AD, Dash S, Babu SV, Jain I (2007) Numerical modeling of cyclone’s impact on the ocean: a case study of Orissa super cyclone. *J Coast Res* 23(5):1245–1250
- SANDS (Shoreline and Nearshore Data System) (2013) SANDS software Version 7.0, CH2M Hill, London, UK
- Sorensen RM (2006) Basic coastal engineering, 3rd edn. Wiley, Chichester
- Sundar V (1986) Wave characteristics off the south east coast of India. *Ocean Eng* 13(4):327–338
- Suresh RRV, Annapurnaiah K, Reddy KG, Lakshmi TN, Balakrishnan Nair TM (2010) Wind sea and Swell Characteristics off East coast of India during Southwest Monsoon. *Int J Oceans Oceanogr* 4(1):35–44
- Wang DW, Hwang PA (2001) An operational method for separating wind sea and swell from ocean wave spectra. *J Atmos Oceanic Technol* 18:2052–2062
- Webster PJ (2008) Myanmar’s deadly daffodil. *Nat Geosci* 1(8):488–490
- Young IR (1999) Wind generated ocean waves. In: Bhattacharyya R, McCormick ME (eds) Elsevier Ocean Engineering Book Series, vol 2. Elsevier, Amsterdam